

## 5. DYNAMICAL THEORY AND ITS APPLICATIONS

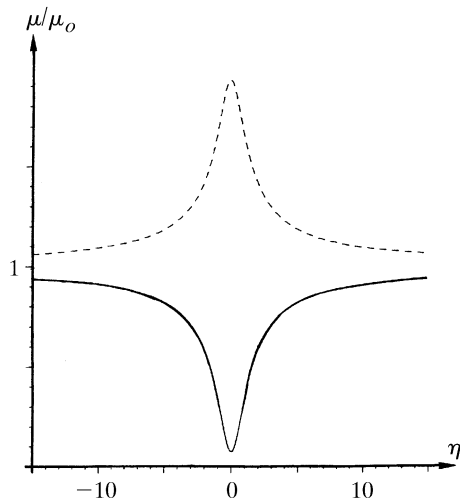


Fig. 5.1.6.1. Variation of the effective absorption with the deviation parameter in the transmission case for the 400 reflection of GaAs using Cu  $K\alpha$  radiation. Solid curve: branch 1; broken curve: branch 2.

nodes of the electric field lie on the planes corresponding to the maxima of the  $hkl$  component of the electron density, the wavefields are absorbed anomalously less than when there is no diffraction. Just the opposite occurs for branch 2 wavefields, whose anti-nodes lie on the maxima of the electron density and which are absorbed more than normal.

The effective absorption coefficient  $\mu$  is related to the imaginary part of the wavevectors through (5.1.2.19),

$$\mu = -4\pi\gamma_o K_{oi},$$

and to the imaginary part of the ratio of the amplitude of the reflected to the incident wave through

$$\mu = \mu_o - 4\pi X_{oi}, \quad (5.1.5.1)$$

where  $X_{oi}$  is the imaginary part of  $X_o$ , which, using (5.1.2.24) and (5.1.3.10), is given by

$$X_o = R\lambda |C| S(\gamma_h) (F_h F_{\bar{h}})^{1/2} \times \{ \eta \pm [\eta^2 + S(\gamma_h)]^{1/2} \} / [2\pi V(|\gamma|)^{1/2}]. \quad (5.1.5.2)$$

Taking the upper sign (+) for the  $\pm$  term corresponds to tie points on branch 1 and taking the lower sign (–) corresponds to tie points on branch 2.

The calculation of the imaginary part  $X_{oi}$  is different in the Laue and in the Bragg cases. In the former case, the imaginary part of  $(\eta^2 + 1)^{1/2}$  is small and can be approximated while in the latter, the imaginary part of  $(\eta^2 - 1)^{1/2}$  is large when the real part of the deviation parameter,  $\eta_r$ , lies between 1 and –1, and cannot be calculated using the same approximation.

### 5.1.6. Intensities of plane waves in transmission geometry

#### 5.1.6.1. Absorption coefficient

In transmission geometry, the imaginary part of  $X_o$  is small and, using a first-order approximation for the expansion of  $(\eta^2 + 1)^{1/2}$ , (5.1.5.1) and (5.1.5.2), the effective absorption coefficient in the absorption case is

$$\mu_j = \mu_o \left[ \frac{1}{2}(1 + \gamma^{-1}) \mp \frac{(\eta_r/2)(1 - \gamma^{-1}) + |C|(\gamma^{-1})^{1/2} |F_{ih}/F_{io}| \cos \varphi}{(\eta_r^2 + 1)^{1/2}} \right], \quad (5.1.6.1)$$

where  $\varphi = \varphi_{rh} - \varphi_{ih}$  is the phase difference between  $F_{rh}$  and  $F_{ih}$  [equation (5.1.2.10)], the upper sign (–) for the  $\mp$  term corresponds to branch 1 and the lower sign (+) corresponds to branch 2 of the dispersion surface. In the symmetric Laue case ( $\gamma = 1$ , reflecting planes normal to the crystal surface), equation (5.1.6.1) reduces to

$$\mu_j = \mu_o \left[ 1 \mp \frac{|C| |F_{ih}/F_{io}| \cos \varphi}{(\eta_r^2 + 1)^{1/2}} \right].$$

Fig. 5.1.6.1 shows the variations of the effective absorption coefficient  $\mu_j$  with  $\eta_r$  for wavefields belonging to branches 1 and 2 in the case of the 400 reflection of GaAs with Cu  $K\alpha$  radiation. It can be seen that for  $\eta_r = 0$  the absorption coefficient for branch 1 becomes significantly smaller than the normal absorption coefficient,  $\mu_o$ . The minimum absorption coefficient,  $\mu_o(1 - |CF_{ih}/F_{io}| \cos \varphi)$ , depends on the nature of the reflection through the structure factor and on the temperature through the Debye–Waller factor included in  $F_{ih}$  [equation (5.1.2.10b)] (Ohtsuki, 1964, 1965). For instance, in diamond-type structures, it is smaller for reflections with even indices than for reflections with odd indices. The influence of temperature is very important when  $|F_{ih}/F_{io}|$  is close to one; for example, for germanium 220 and Mo  $K\alpha$  radiation, the minimum absorption coefficient at 5 K is reduced to about 1% of its normal value,  $\mu_o$  (Ludewig, 1969).

#### 5.1.6.2. Boundary conditions for the amplitudes at the entrance surface – intensities of the reflected and refracted waves

Let us consider an infinite plane wave incident on a crystal plane surface of infinite lateral extension. As has been shown in Section 5.1.3, two wavefields are excited in the crystal, with tie points  $P_1$  and  $P_2$ , and amplitudes  $D_{o1}$ ,  $D_{h1}$  and  $D_{o2}$ ,  $D_{h2}$ , respectively. Maxwell's boundary conditions (see Section A5.1.1.2 of the Appendix) imply continuity of the tangential component of the electric field and of the normal component of the electric displacement across the boundary. Because the index of refraction is so close to unity, one can assume to a very good approximation that there is continuity of the three components of both the electric field and the electric displacement. As a consequence, it can easily be shown that, along the entrance surface, for all components of the electric displacement

$$\begin{aligned} D_o^{(a)} &= D_{o1} + D_{o2} \\ 0 &= D_{h1} + D_{h2}, \end{aligned} \quad (5.1.6.2)$$

where  $D_o^{(a)}$  is the amplitude of the incident wave.

Using (5.1.3.11), (5.1.5.2) and (5.1.6.2), it can be shown that the intensities of the four waves are

$$|D_{oj}|^2 = |D_o^{(a)}|^2 \exp(-\mu_j z/\gamma_o) \left[ (1 + \eta_r^2)^{1/2} \mp \eta_r \right]^2 \times [4(1 + \eta_r^2)]^{-1}, \quad (5.1.6.3)$$

$$|D_{hj}|^2 = |D_o^{(a)}|^2 \exp(-\mu_j z/\gamma_o) |F_h/F_{\bar{h}}| [4\gamma(1 + \eta_r^2)]^{-1};$$

top sign:  $j = 1$ ; bottom sign:  $j = 2$ .

## 5.1. DYNAMICAL THEORY OF X-RAY DIFFRACTION

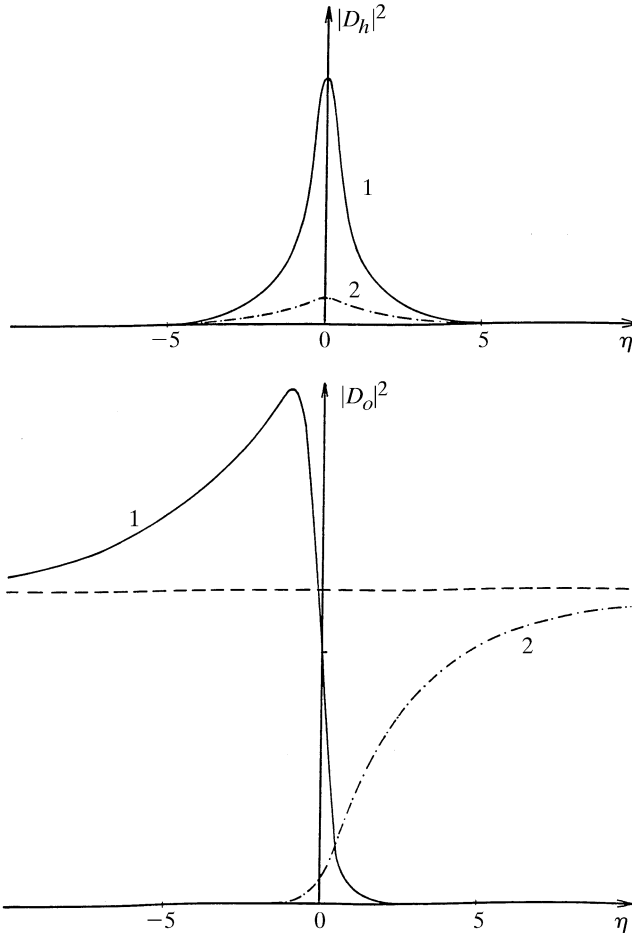


Fig. 5.1.6.2. Variation of the intensities of the reflected and refracted waves in an absorbing crystal for the 220 reflection of Si using Mo  $K\alpha$  radiation,  $t = 1$  mm ( $\mu t = 1.42$ ). Solid curve: branch 1; dashed curve: branch 2.

Fig. 5.1.6.2 represents the variations of these four intensities with the deviation parameter. Far from the reflection domain,  $|D_{h1}|^2$  and  $|D_{h2}|^2$  tend toward zero, as is normal, while

$$\begin{aligned} |D_{o1}|^2 &\gg |D_{o2}|^2 \text{ for } \eta_r \Rightarrow -\infty, \\ |D_{o1}|^2 &\ll |D_{o2}|^2 \text{ for } \eta_r \Rightarrow +\infty. \end{aligned}$$

This result shows that the wavefield of highest intensity ‘jumps’ from one branch of the dispersion surface to the other across the reflection domain. This is an important property of dynamical theory which also holds in the Bragg case and when a wavefield crosses a highly distorted region in a deformed crystal [the so-called *interbranch scattering*: see, for instance, Authier & Balibar (1970) and Authier & Malgrange (1998)].

### 5.1.6.3. Boundary conditions at the exit surface

#### 5.1.6.3.1. Wavevectors

When a wavefield reaches the exit surface, it breaks up into two constituent waves. Their wavevectors are obtained by applying again the condition of the continuity of their tangential components along the crystal surface. The extremities,  $M_j$  and  $N_j$ , of these wavevectors

$$\mathbf{OM}_j = \mathbf{K}_{oj}^{(d)} \quad \mathbf{HN}_j = \mathbf{K}_{hj}^{(d)}$$

lie at the intersections of the spheres of radius  $k$  centred at  $O$  and  $H$ , respectively, with the normal  $\mathbf{n}'$  to the crystal exit surface drawn from  $P_j$  ( $j = 1$  and  $2$ ) (Fig. 5.1.6.3).

If the crystal is wedge-shaped and the normals  $\mathbf{n}$  and  $\mathbf{n}'$  to the entrance and exit surfaces are not parallel, the wavevectors of the waves generated by the two wavefields are not parallel. This effect is due to the refraction properties associated with the dispersion surface.

#### 5.1.6.3.2. Amplitudes – Pendellösung

We shall assume from now on that the crystal is plane parallel. Two wavefields arrive at any point of the exit surface. Their constituent waves interfere and generate emerging waves in the refracted and reflected directions (Fig. 5.1.6.4). Their respective amplitudes are given by the boundary conditions

$$\begin{aligned} D_o^{(d)} \exp(-2\pi i \mathbf{K}_o^{(d)} \cdot \mathbf{r}) &= D_{o1} \exp(-2\pi i \mathbf{K}_{o1} \cdot \mathbf{r}) \\ &\quad + D_{o2} \exp(-2\pi i \mathbf{K}_{o2} \cdot \mathbf{r}) \\ D_h^{(d)} \exp(-2\pi i \mathbf{K}_h^{(d)} \cdot \mathbf{r}) &= D_{h1} \exp(-2\pi i \mathbf{K}_{h1} \cdot \mathbf{r}) \\ &\quad + D_{h2} \exp(-2\pi i \mathbf{K}_{h2} \cdot \mathbf{r}), \end{aligned} \quad (5.1.6.4)$$

where  $\mathbf{r}$  is the position vector of a point on the exit surface, the origin of phases being taken at the entrance surface.

In a plane-parallel crystal, (5.1.6.4) reduces to

$$\begin{aligned} D_o^{(d)} &= D_{o1} \exp(-2\pi i \overline{MP}_1 \cdot t) + D_{o2} \exp(-2\pi i \overline{MP}_2 \cdot t) \\ D_h^{(d)} &= D_{h1} \exp(-2\pi i \overline{MP}_1 \cdot t) + D_{h2} \exp(-2\pi i \overline{MP}_2 \cdot t), \end{aligned}$$

where  $t$  is the crystal thickness.

In a *non-absorbing* crystal, the amplitudes squared are of the form

$$|D_o^{(d)}|^2 = |D_{o1}|^2 + |D_{o2}|^2 + 2D_{o1}D_{o2} \cos 2\pi \overline{P_2P_1}t.$$

This expression shows that the intensities of the refracted and reflected beams are oscillating functions of crystal thickness. The period of the oscillations is called the *Pendellösung* distance and is

$$\Lambda = 1/\overline{P_2P_1} = \Lambda_L/(1 + \eta_r^2)^{1/2}.$$

#### 5.1.6.4. Reflecting power

For an *absorbing* crystal, the intensities of the reflected and refracted waves are

$$\begin{aligned} |D_o^{(d)}|^2 &= |D_o^{(a)}|^2 A_\eta \left\{ \cosh(2\nu + \mu_a t) \right. \\ &\quad \left. + \cos[2\pi t \Lambda^{-1} - 2\eta_i(1 + \eta_r^2)^{-1/2}] \right\} \\ |D_h^{(d)}|^2 &= |D_o^{(a)}|^2 |F_h/F_h| \gamma^{-1} A_\eta [\cosh(\mu_a t) - \cos(2\pi t \Lambda^{-1})], \end{aligned} \quad (5.1.6.5)$$

where

$$\begin{aligned} A_\eta &= [\exp -\mu_o t (\gamma_o^{-1} + \gamma_h^{-1})] / 2(1 + \eta_r^2), \\ \mu_a &= \mu_j \left[ 1/2(\gamma_o^{-1} - \gamma_h^{-1}) \eta_r \right. \\ &\quad \left. + |C| |F_{ih}/F_{io}| \cos \varphi / (\gamma_o \gamma_h)^{1/2} \right] (1 + \eta_r^2)^{-1/2}, \\ \nu &= \arg \sinh \eta_r \end{aligned}$$

and  $\mu_j$  is given by equation (5.1.6.1).

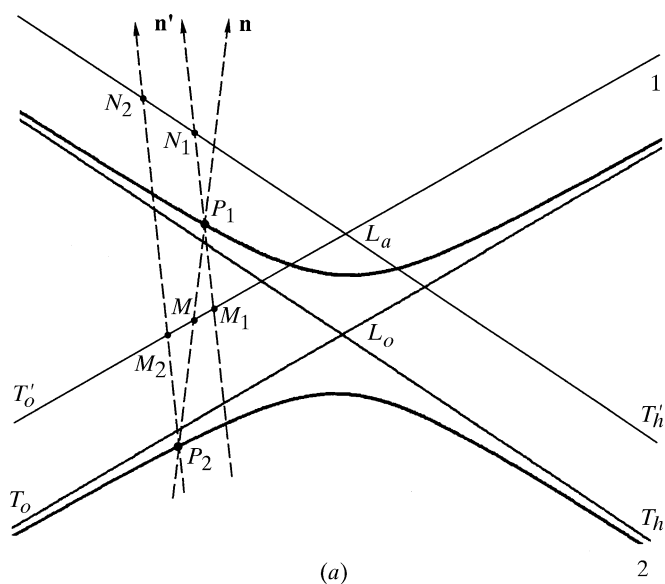


Fig. 5.1.6.3. Boundary condition for the wavevectors at the exit surface. (a) Reciprocal space. The wavevectors of the emerging waves are determined by the intersections  $M_1$ ,  $M_2$ ,  $N_1$  and  $N_2$  of the normals  $\mathbf{n}'$  to the exit surface, drawn from the tie points  $P_1$  and  $P_2$  of the wavefields, with the tangents  $T'_o$  and  $T'_h$  to the spheres centred at  $O$  and  $H$  and of radius  $k$ , respectively. (b) Direct space.

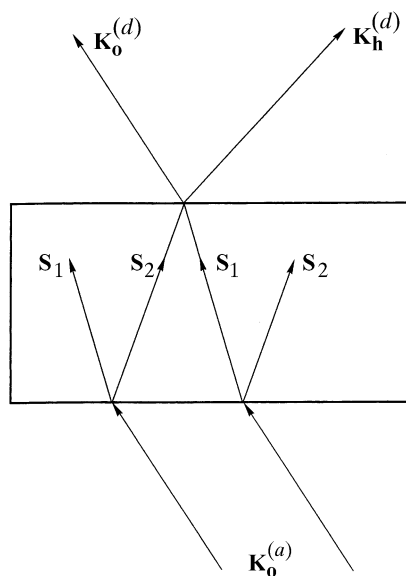


Fig. 5.1.6.4. Decomposition of a wavefield into its two components when it reaches the exit surface.  $\mathbf{S}_1$  and  $\mathbf{S}_2$  are the Poynting vectors of the two wavefields propagating in the crystal belonging to branches 1 and 2 of the dispersion surface, respectively, and interfering at the exit surface.

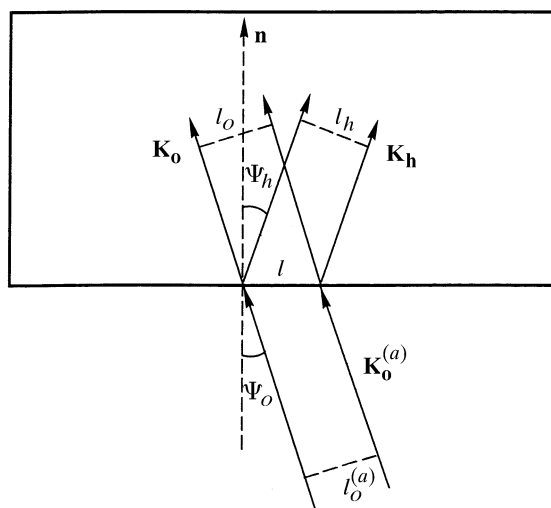


Fig. 5.1.6.5. Cross sections of the incident,  $\mathbf{K}_o^{(a)}$ , refracted,  $\mathbf{K}_o$ , and reflected,  $\mathbf{K}_h$ , waves.

Depending on the absorption coefficient, the cosine terms are more or less important relative to the hyperbolic cosine term and the oscillations due to *Pendellösung* have more or less contrast.

For a non-absorbing crystal, these expressions reduce to

$$|D_o^{(d)}|^2 = |D_o^{(a)}|^2 \left[ \frac{1 + 2\eta^2 + \cos(2\pi t \Lambda^{-1})}{2(1 + \eta_r^2)} \right], \quad (5.1.6.6)$$

$$|D_h^{(d)}|^2 = |D_o^{(a)}|^2 \left[ \frac{1 - \cos(2\pi t \Lambda^{-1})}{2\gamma(1 + \eta_r^2)} \right].$$

What is actually measured in a counter receiving the reflected or the refracted beam is the *reflecting power*, namely the ratio of the energy of the reflected or refracted beam on the one hand and the energy of the incident beam on the other. The energy of a beam is obtained by multiplying its intensity by its cross section. If  $l$  is the width of the trace of the beam on the crystal surface, the cross sections of the incident (or refracted) and reflected beams are proportional to (Fig. 5.1.6.5)  $l_o = l\gamma_o$  and  $l_h = l\gamma_h$ , respectively.

The reflecting powers are therefore:

$$\text{Refracted beam: } I_o = l_o |D_o^{(d)}|^2 / l_o |D_o^{(a)}|^2 = |D_o^{(d)}|^2 / |D_o^{(a)}|^2,$$

$$\text{Reflected beam: } I_h = l_h |D_h^{(d)}|^2 / l_o |D_o^{(a)}|^2 = \gamma |D_h^{(d)}|^2 / |D_o^{(a)}|^2. \quad (5.1.6.7)$$

Using (5.1.6.6), it is easy to check that  $I_o + I_h = 1$  in the non-absorbing case; that is, that conservation of energy is satisfied. Equations (5.1.6.6) show that there is a periodic exchange of energy between the refracted and the reflected waves as the beam penetrates the crystal; this is why Ewald introduced the expression *Pendellösung*.

The oscillations in the rocking curve were first observed by Lefeld-Sosnowska & Malgrange (1968, 1969). Their periodicity can be used for accurate measurements of the form factor [see, for instance, Bonse & Teworte (1980)]. Fig. 5.1.6.6 shows the shape of the rocking curve for various values of  $t/\Lambda_L$ .

The *width at half-height of the rocking curve*, averaged over the *Pendellösung* oscillations, corresponds in the non-absorbing case to  $\Delta\eta = 2$ , that is, to  $\Delta\theta = 2\delta$ , where  $\delta$  is given by (5.1.3.6).

## 5.1. DYNAMICAL THEORY OF X-RAY DIFFRACTION

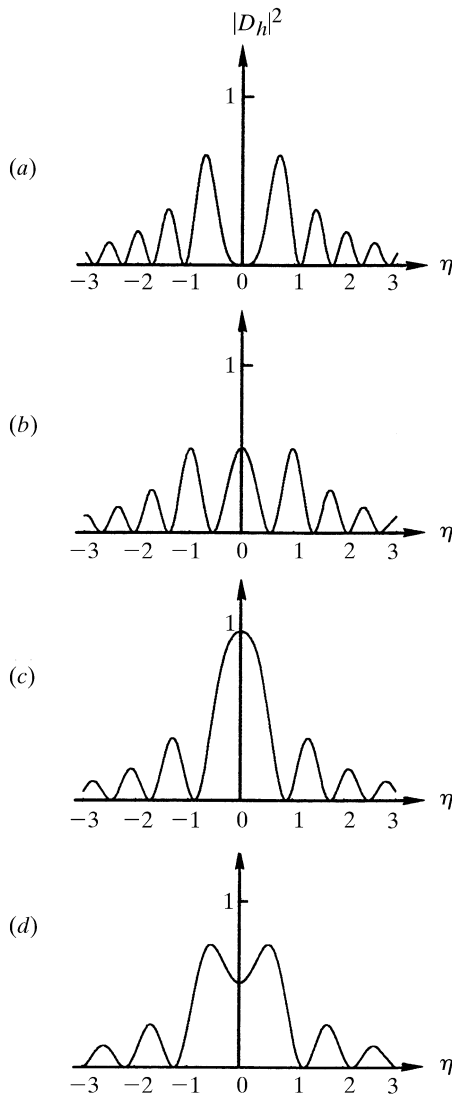


Fig. 5.1.6.6. Theoretical rocking curves in the transmission case for non-absorbing crystals and for various values of  $t/\Lambda_L$ : (a)  $t/\Lambda_L = 1.25$ ; (b)  $t/\Lambda_L = 1.5$ ; (c)  $t/\Lambda_L = 1.75$ ; (d)  $t/\Lambda_L = 2.0$ .

### 5.1.6.5. Integrated intensity

#### 5.1.6.5.1. Non-absorbing crystals

The integrated intensity is the ratio of the total energy recorded in the counter when the crystal is rocked to the intensity of the incident beam. It is proportional to the area under the line profile:

$$I_{hi} = \int_{-\infty}^{+\infty} I_h d(\Delta\theta). \quad (5.1.6.8)$$

The integration was performed by von Laue (1960). Using (5.1.3.5), (5.1.6.6) and (5.1.6.7) gives

$$I_{hi} = A \int_0^{2\pi\Lambda_L^{-1}} J_0(z) dz,$$

where  $J_0(z)$  is the zeroth-order Bessel function and

$$A = \frac{R\lambda^2 |CF_h|(\gamma)^{1/2}}{2V \sin 2\theta}.$$

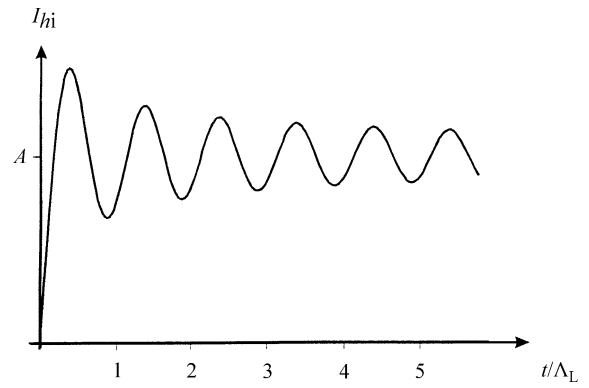


Fig. 5.1.6.7. Variations with crystal thickness of the integrated intensity in the transmission case (no absorption) (arbitrary units). The expression for  $A$  is given in the text.

Fig. 5.1.6.7 shows the variations of the integrated intensity with  $t/\Lambda_L$ .

#### 5.1.6.5.2. Absorbing crystals

The integration was performed for absorbing crystals by Kato (1955). The integrated intensity in this case is given by

$$I_{hi} = A |F_h/F_{\bar{h}}| \exp[-1/2\mu_o t(\gamma_o^{-1} + \gamma_h^{-1})] \times \left[ \int_0^{2\pi\Lambda_L^{-1}} J_0(z) dz - 1 + I_0(\zeta) \right],$$

where

$$\zeta = \mu_o t \left\{ [ |C|^2 |F_{ih}/F_{io}|^2 \cos^2 \varphi + (\gamma_h - \gamma_o)/(4\gamma_o\gamma_h) ] / (\gamma_o\gamma_h) \right\}^{1/2}$$

and  $I_0(\zeta)$  is a modified Bessel function of zeroth order.

#### 5.1.6.6. Thin crystals – comparison with geometrical theory

Using (5.1.6.6) and (5.1.6.7), the reflecting power of the reflected beam may also be written

$$I_h = \pi^2 t^2 \Lambda_o^{-2} f(\eta),$$

where

$$f(\eta) = \left[ \frac{\sin U(1 + \eta^2)^{1/2}}{U(1 + \eta^2)^{1/2}} \right]^2$$

and

$$U = \pi t \Lambda_o^{-1}.$$

When  $t\Lambda_o^{-1}$  is very small,  $f(\eta)$  tends asymptotically towards the function

$$f_1(\eta) = \left[ \frac{\sin U\eta}{U\eta} \right]^2$$

and  $I_h$  towards the value given by geometrical theory. The condition for geometrical theory to apply is, therefore, that the crystal thickness be much smaller than the *Pendellösung* distance. In practice, the two theories agree to within a few per cent for a

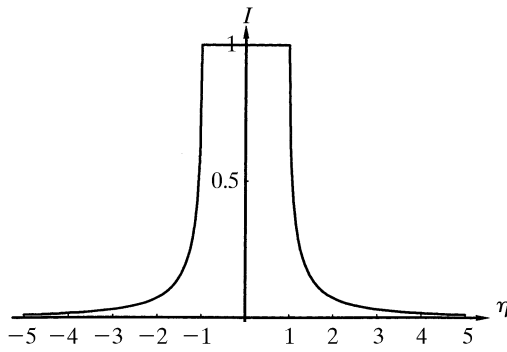


Fig. 5.1.7.1. Theoretical rocking curve in the reflection case for a non-absorbing thick crystal in terms of the deviation parameter.

crystal thickness smaller than or equal to a third of the *Pendelösung* distance [see Authier & Malgrange (1998)].

### 5.1.7. Intensity of plane waves in reflection geometry

#### 5.1.7.1. Thick crystals

##### 5.1.7.1.1. Non-absorbing crystals

*Rocking curve.* The geometrical construction in Fig. 5.1.3.5 shows that, in the Bragg case, the normal to the crystal surface drawn from the extremity of the incident wavevector intersects the dispersion surface either at two points of the same branch,  $P_1, P'_1$ , for branch 1,  $P_2, P'_2$  for branch 2, or at imaginary points. It was shown in Section 5.1.2.6 that the propagation of the wavefields inside the crystal is along the normal to the dispersion surface at the corresponding tie points. Fig. 5.1.3.5 shows that this direction is oriented towards the outside of the crystal for tie points  $P'_1$  and  $P'_2$ . In a very thick crystal, these wavefields cannot exist because there is always a small amount of absorption. One concludes that in the thick-crystal case and in reflection geometry, only one wavefield is excited inside the crystal. It corresponds to branch 1 on the low-angle side of the rocking curve and to branch 2 on the high-angle side. Using the same approximations as in Section 5.1.6.2, the amplitude  $\mathbf{D}_h^{(a)}$  of the wave reflected at the crystal surface is obtained by applying the boundary conditions, which are particularly simple in this case:

$$\mathbf{D}_o = \mathbf{D}_o^{(a)}, \quad \mathbf{D}_h^{(a)} = \mathbf{D}_h.$$

The reflecting power is given by an expression similar to (5.1.6.7):

$$I_h = |\gamma| |\xi_j|^2,$$

where the expression for  $\xi_j$  is given by (5.1.3.12), and  $j = 1$  or  $2$  depending on which wavefield propagates towards the inside of the crystal. When the normal to the entrance surface intersects the dispersion surface at imaginary points, *i.e.* when  $-1 < \eta < +1$ ,

$$|\xi|^2 = |\gamma|^{-1}, \quad I_h = 1, \quad (5.1.7.1)$$

and there is *total reflection*. Outside the total-reflection domain, the reflecting power is given by

$$I_h = [|\eta| - (\eta^2 - 1)^{1/2}]^2. \quad (5.1.7.2)$$

The rocking curve has the well known top-hat shape (Fig. 5.1.7.1). Far from the total-reflection domain, the curve can be approximated by the function

$$I_h \simeq 1/(4\eta^2).$$

*Width of the total-reflection domain.* The width of the total-reflection domain is equal to  $\Delta\eta = 2$  and its angular width is therefore equal, using (5.1.3.5), to  $2\delta$ , where  $\delta$  is given by (5.1.3.6). It is proportional to the structure factor, the polarization factor  $C$  and the square root of the asymmetry factor  $|\gamma|$ . Using an asymmetric reflection, it is therefore possible to decrease the width at will. This is used in monochromators to produce a pseudo plane wave [see, for instance, Kikuta & Kohra (1970)]. It is possible to deduce the value of the form factor from very accurate measurements of the rocking curve; see, for instance, Kikuta (1971).

*Integrated intensity.* The integrated intensity is defined by (5.1.6.8):

$$I_{hi} = 8\delta/3. \quad (5.1.7.3)$$

*Penetration depth.* Within the domain of total reflection, there are two wavefields propagating inside the crystal with imaginary wavevectors, one towards the inside of the crystal and the other one in the opposite direction, so that they cancel out and, globally, no energy penetrates the crystal. The absorption coefficient of the waves penetrating the crystal is

$$\mu = -4\pi K_{oi}\gamma_o = 2\pi\gamma_o(1 - \eta^2)^{1/2}/\Lambda_B, \quad (5.1.7.4)$$

where  $\Lambda_B$  is the value taken by  $\Lambda_o$  [equation (5.1.3.8)] in the Bragg case.

The penetration depth is a minimum at the middle of the reflection domain and at this point it is equal to  $\Lambda_B/2\pi$ . This attenuation effect is called *extinction*, and  $\Lambda_B$  is called the *extinction length*. It is a specific property owing to the existence of wavefields. The resulting propagation direction of energy is parallel to the crystal surface, but with a cross section equal to zero: it is an *evanescent wave* [see, for instance, Cowan *et al.* (1986)].

##### 5.1.7.1.2. Absorbing crystals

*Rocking curve.* Since the sign of  $\gamma$  is negative,  $[\eta^2 + S(\gamma h)]^{1/2}$  in (5.1.3.10) has a very large imaginary part when  $|\eta_r| \leq 1$ . It cannot be calculated using the same approximations as in the Laue case. Let us set

$$Z \exp(i\Psi') = \eta \mp (\eta^2 - 1)^{1/2}. \quad (5.1.7.5)$$

The reflecting power is

$$I_h = (F_h/F_h')^{1/2} Z^2, \quad (5.1.7.6)$$

where  $Z = [L - (L^2 - 1)^{1/2}]^{1/2}$ ,  $L = |\eta|^2 + \rho^2$  and  $\rho = |\eta^2 - 1|$  is the modulus of expression (5.1.7.5) where the sign is chosen in such a way that  $Z$  is smaller than 1.

The expression for the reflected intensity in the absorbing Bragg case was first given by Prins (1930). The way of representing it given here was first used by Hirsch & Ramachandran (1950). The properties of the rocking curve have been described by Fingerland (1971).

There is no longer a total-reflection domain and energy penetrates the crystal at all incidence angles, although with a very